



Cite this: *Org. Biomol. Chem.*, 2021, **19**, 6397

Received 31st May 2021,
Accepted 5th July 2021

DOI: 10.1039/d1ob01053k

rsc.li/obc

Chalcogen bonding mediates the formation of supramolecular helices of azapeptides in crystals†

Di Shi, Jinlian Cao, Peimin Weng, Xiaosheng Yan, * Zhao Li and Yun-Bao Jiang *

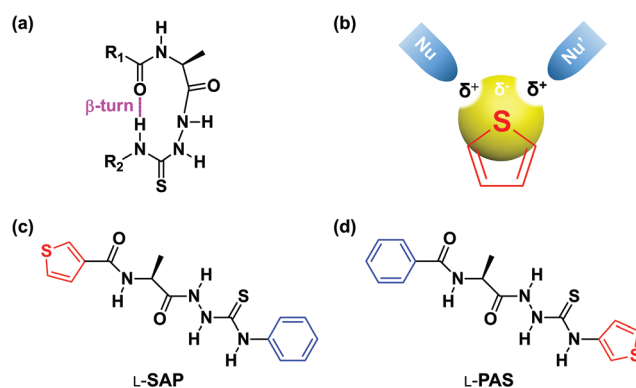
To explore whether chalcogen bonding was able to drive the formation of supramolecular helices, alanine-based azapeptides containing a β -turn structure, with a thiophene group, respectively, incorporated in the *N*- or *C*-terminus, were employed as helical building blocks. While the former derivative formed a supramolecular *M*-helix via intermolecular S...S chalcogen bonding in crystals, the latter formed *P*-helix via intermolecular S...O chalcogen bonding.

Chalcogen bonding is an attractive interaction that occurs between a positively polarized chalcogen atom and a nucleophile.¹ It has been known for several decades,² yet remains largely unutilized. A chalcogen bond shares many similarities with a halogen bond that occurs between a positively polarized halogen atom and a nucleophile,³ such as positive σ -holes, high directionality and high strength.^{4,5} Extensive research has been performed on the utilization of halogen bonding^{6,7} in crystal engineering,⁸ molecular recognition,⁹ transport,¹⁰ catalysis,¹¹ organic frameworks¹² and supramolecular helical assembly.^{13–16} We recently created halogen-bonding-driven supramolecular helices by employing folded short azapeptide containing β -turns (alanine-based *N*-amidothiourea, Scheme 1a) as helical fragments.^{14–16} It was found that the propagation of the helicity of the building block enhances the intermolecular halogen bonding and thus promotes the formation of supramolecular helices in both the solid state and solution phase.^{14,15}

Probably inspired by the impressive developments of the halogen bond, the utilization of chalcogen bonds has recently been brought into focus, for example, in crystal engineering,¹⁷ anion recognition¹⁸ and transport,¹⁹ and catalysis.²⁰ We there-

fore initiated our efforts in developing chalcogen bonding as an alternative driving force to build supramolecular helices, a subject that has not been well explored.

We chose a folded short azapeptide containing a helical β -turn structure as a structural framework of the building block for our exploration of chalcogen bonding-driven formation of a supramolecular helix. This is not only because of our successful efforts in creating supramolecular helices using building blocks of that structure employing halogen bonding,^{14–16} but also because of its good crystallinity that we noted during our explorations on these helical azapeptides, which makes it possible to allow the characterization of the supramolecular helical structures by crystal structural analysis.^{21,22} We also observed that in such azapeptides (Scheme 1a), S and O atoms in an amidothiourea motif that do not take part in the intramolecular hydrogen bonding are nucleophiles available for chalcogen bonding as acceptors. We therefore introduced a thiophene group, a well-known chalc-



Scheme 1 (a) β -Turn structure in alanine-based *N*-amidothiourea (azapeptide). Dashed pink line highlights the intramolecular ten-membered ring hydrogen bond leading to a β -turn structure. (b) Chalcogen bonding of thiophene. (c and d) Chemical structures of alanine-based *N*-amidothioureas with the thiophene group attached at *N*- (L-SAP, c) and *C*-terminii (L-PAS, d), respectively.

Department of Chemistry, College of Chemistry and Chemical Engineering, The MOE Key Laboratory of Spectrochemical Analysis and Instrumentation, and iChEM, Xiamen University, Xiamen 361005, China. E-mail: xshyan@xmu.edu.cn, ybjjiang@xmu.edu.cn

† Electronic supplementary information (ESI) available: CCDC 2084138 and 2084139. For ESI and crystallographic data in CIF or other electronic format see DOI: 10.1039/d1ob01053k

gen bonding donor (Scheme 1b),^{4,17,19,23–25} into the *N*- or *C*-terminus of the azapeptide motif, leading to the formation of *L*-SAP and *L*-PAS (Scheme 1c and d). Despite their similar β -turn structures, we find that in the crystals *L*-SAP forms a supramolecular *M*-helix *via* intermolecular S \cdots S chalcogen bonding between the S-atom from thiophene and the S-atom from thiourea groups, while *L*-PAS forms a *P*-helix that is driven by intermolecular S \cdots O chalcogen bonding between the S-atom from thiophene and the O-atom from amidothiourea moieties. Our results therefore demonstrate that chalcogen bonding is indeed capable of driving the formation of supramolecular helices.

L-SAP and *L*-PAS (Scheme 1c and d) were synthesized following procedures described in Schemes S1 and S2.† Their crystals were grown by slow evaporation of the solution samples in 1:1 (v/v) CH₃CN/CH₃OH. Crystal structure data and refinement are presented in Table S1.† Both have a chiral *P*2₁ space group.

The crystal structure of *L*-SAP shows that it adopts a folded conformation with an intramolecular ten-membered ring hydrogen bond (N–H^d \cdots O=C), leading to a type II β -turn structure (Fig. 1a and Table S2†).²⁶ Adjacent two *L*-SAP molecules along the *b*-axis are bridged by one short intermolecular S^h \cdots S^g interaction (Fig. 1b). The S^h \cdots S^g distance is 3.535 Å, shorter than the sum of van der Waals radii of two S atoms (3.600 Å), and the C–S^h \cdots S^g angle is 154.52°. This interaction is therefore identified as chalcogen bonding, with a calculated

Table 1 Structural parameters of the intermolecular chalcogen bonds according to X-ray crystal structures

Crystal	Interaction	Distance ^a (Å)	Angle ^b (°)	ΔE^c (kJ mol ⁻¹)
<i>L</i> -SAP	S ^h \cdots S ^g	3.535	154.52	–54.84
<i>L</i> -PAS	S ^h \cdots O ^f	3.216	170.19	–40.71

^a Distance of S^h \cdots O^f or S^h \cdots S^g. ^b Angle of CS^hO^f or CS^hS^g. ^c Calculated energy using WB97XD DFT with the 6-31+G(d,p) basis set.

interaction energy of –54.84 kJ mol⁻¹ (Table 1). The head-to-tail S^h \cdots S^g chalcogen bonding drives *L*-SAP molecules into the 1D supramolecular helix along the *b*-axis of *M*-helicity and 8.16 Å pitch (Fig. 1c). The helicity led by the β -turn structure is supposed to propagate along the chalcogen bond in the S^h \rightarrow S^g direction. Subsequently, parallel chalcogen-bonded *M*-helices of *L*-SAP are held together through inter-helix N–H^c \cdots O=C and N–H^b \cdots O=C hydrogen bonds (for structural parameters, see Table S3†), leading to a 2D supramolecular helical array along the *a*-axis (Fig. S1†).

The crystal structure of *L*-PAS also reveals a folded conformation containing a type II β -turn structure (Fig. 2a and Table S2†). Instead of the S^h \cdots S^g chalcogen bonds in the supramolecular helix of *L*-SAP, S^h \cdots O^f chalcogen bonds are observed in the crystal structure of *L*-PAS (Fig. 2b). The S^h \cdots O^f distance

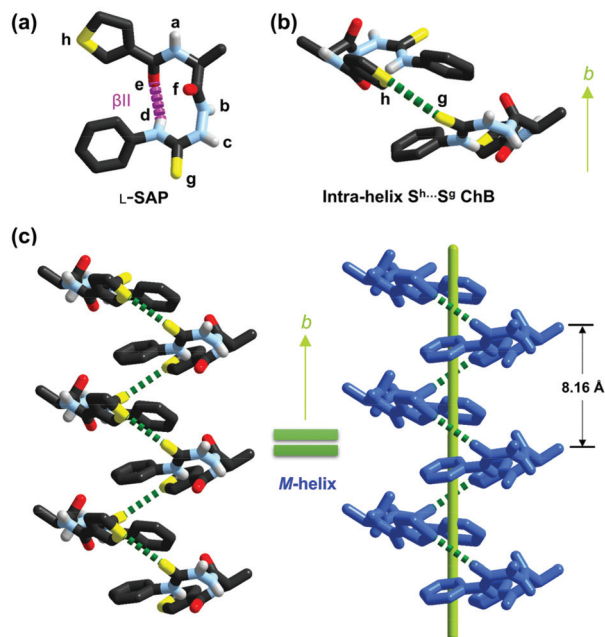


Fig. 1 (a) Crystal structure of *L*-SAP. The dashed pink line highlights the intramolecular ten-membered ring hydrogen bond that is indicative of the β -turn structure. (b) Intermolecular S^h \cdots S^g chalcogen bonding (ChB, dashed green line) between adjacent two *L*-SAP molecules along the *b*-axis. (c) Supramolecular 1D *M*-helix formed from *L*-SAP molecules along the *b*-axis through intermolecular S^h \cdots S^g chalcogen bonding (dashed green lines). For clarity, all –CH protons are omitted.

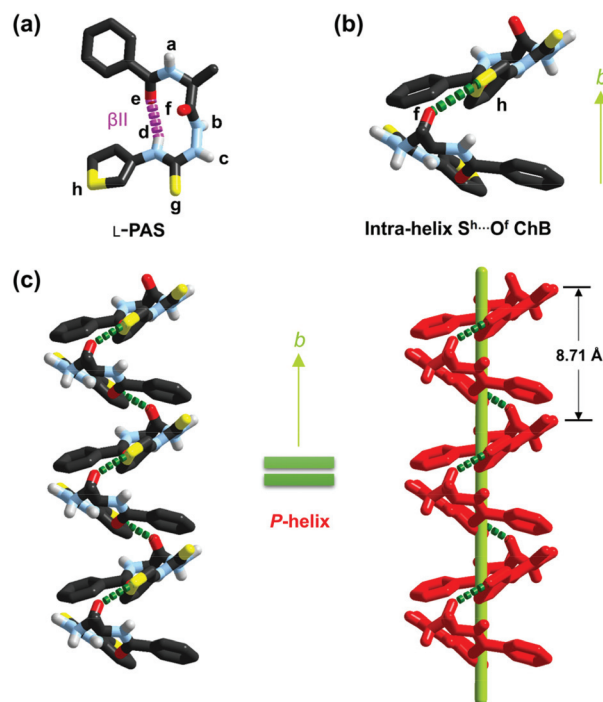


Fig. 2 (a) Crystal structure of *L*-PAS. Dashed pink line highlights the intramolecular ten-membered ring hydrogen bond that leads to a β -turn structure. (b) Intermolecular S^h \cdots O^f chalcogen bond (ChB, dashed green line) between adjacent two *L*-PAS molecules along the *b*-axis. (c) Supramolecular 1D *P*-helix of *L*-PAS molecules along the *b*-axis *via* intermolecular S^h \cdots O^f chalcogen bonding (dashed green lines). For clarity, all –CH protons are omitted.

is 3.216 Å, smaller than the sum of van der Waals radii of S and O atoms (3.320 Å), while the angle of C–S^h...O^f of 170.19° indicates that it is almost linear. The interaction energy of the S^h...O^f chalcogen bond was calculated to be *ca.* –40.71 kJ mol^{–1} (Table 1). Along the *b*-axis, head-to-tail S^h...O^f chalcogen bonding bridges L-PAS molecules into a 1D supramolecular *P*-helix of 8.71 Å pitch (Fig. 2c), along which the helicity of the β-turn structure is propagated. The supramolecular 2D helical array is formed because of the inter-helix N–H^c...O=C and N–H^b...O=C hydrogen bonds (Table S3†) that link parallel chalcogen-bonded *P*-helices of L-PAS along the *a*-axis (Fig. S2†). In addition, one equivalent solvent CH₃CN molecule is embedded in the 2D supramolecular helical network *via* N–H^a...N≡C hydrogen bonds (Fig. S2†).

It is interesting to note that, despite the same L-alanine residue and a similar βII turn structure, L-SAP and L-PAS form supramolecular helices of opposite handedness, *M*- and *P*-helix, respectively, *via* different intermolecular chalcogen bonding interactions, S^h...S^g versus S^h...O^f. It is shown in biotic helices that an α-helix composed of L-α-amino acid residues is right-handed (*P*-helix),²⁷ while peptides composed of L-β-amino acid residues fold into a 3₁₄-*M*-helix.^{28,29} This means that an identical chiral configuration does not prefigure a unique helix handedness, the same as our observations suggest. CD spectra of the L-SAP and L-PAS crystals show opposite CD signals at a long wavelength window of 280–300 nm (Fig. 3a), consistent with the opposite handedness of their supramolecular helices.

We further rationalize the differences in the chalcogen bonding and opposite handedness of the helices from L-SAP and L-PAS (Fig. 4). In these two azapeptide molecules, the S^h atom from the thiophene group is the chalcogen bonding donor, while S^g or O^f atoms of the amidothiourea moiety are potential chalcogen bonding acceptors, allowing S^h...S^g or S^h...O^f chalcogen bonding. Note that the O^e-atom of the *N*-terminal amide group takes part in the intramolecular hydrogen bonding for β-turns, and it is unable to participate in the intermolecular chalcogen bonding. For L-SAP with *N*-terminal thiophene, the intermolecular S^h...S^g interaction

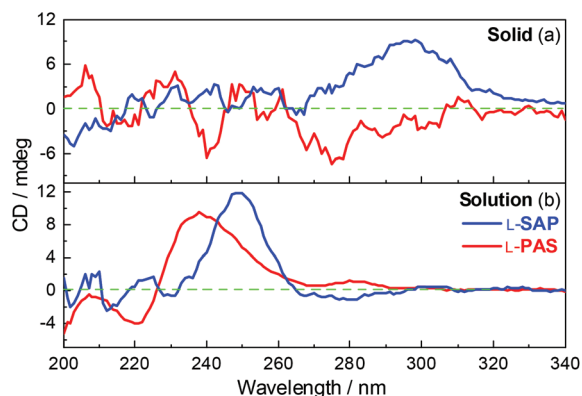


Fig. 3 CD spectra of L-SAP and L-PAS in the crystalline solid state (a) and in CH₃CN solution (b). The concentration of the solid CD sample is about 1.0 mg per 100 mg KBr. [L-SAP] = [L-PAS] = 40 μM in CH₃CN.

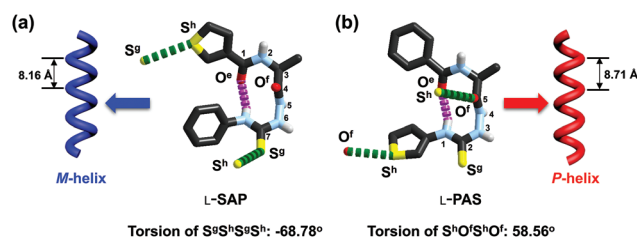


Fig. 4 (a) In L-SAP crystals, the S^h...S^g chalcogen bonding allows 7 atoms of the β-turn motif to be involved in the helix. The torsion of two consecutive S^h...S^g chalcogen bonds (S^gS^hS^gS^h) is –68.78°, indicative of the *M*-helicity. (b) In L-PAS crystals, the S^h...O^f chalcogen bonding allows 5 atoms of the β-turn motif to be involved in the helix. The torsion of two consecutive S^h...O^f chalcogen bonds (S^hO^fS^hO^f) is 58.56°, indicative of the *P*-helicity.

allows more atoms of the β-turn structure to be involved in the helical chain compared to that by the alternative S^h...O^f interaction (7 *vs.* 4 atoms), facilitating to a higher extent the propagation of the helicity of the β-turn structure and thereby the formation of a supramolecular helix (Fig. 4a). In contrast, for L-PAS in which the thiophene moiety is attached at the *C*-terminus, the S^h...S^g interaction would involve much less of the β-turn structure in the helix than that by the S^h...O^f interaction (2 *vs.* 5 atoms, Fig. 4b). The calculated energy indicates that the S^h...S^g chalcogen bonding in L-SAP crystals is stronger than the S^h...O^f chalcogen bonding in L-PAS crystals (–54.84 *vs.* –40.71 kJ mol^{–1}, Table 1), presumably because in the former case more atoms of the β-turn structure are involved in the helix than that in the latter (7 *vs.* 5 atoms, Fig. 4), which therefore results in a more efficient propagation of the helicity of the building block during the formation of the supramolecular helix. This explains the observed shorter pitch of the *M*-helix of L-SAP than that of the *P*-helix of L-PAS (8.16 *vs.* 8.71 Å, Fig. 1c and 2c).³⁰

Different intermolecular chalcogen bonding patterns would propagate the helicity of the β-turn structure along different directions that may lead to opposite helical handedness. Indeed, the torsion of two consecutive S^h...S^g chalcogen bonds in L-SAP crystals (S^gS^hS^gS^h) is –68.78°, indicative of the *M*-helicity of the supramolecular helix, while it is 58.56° for two S^h...O^f chalcogen bonds in L-PAS crystals (S^hO^fS^hO^f), which indicates *P*-helicity (Fig. 4), as those observed in the crystal structures of L-SAP (Fig. 1c) and L-PAS (Fig. 2c). Our results therefore confirm that chalcogen bonding could drive the formation of the supramolecular helix from a helical building block.

¹H NMR spectra of L-SAP and L-PAS in CD₃CN exhibit a set of well-resolved signals (Fig. S3†), identical to those recorded from samples made by dissolving crystals of L-SAP and L-PAS in CD₃CN (Fig. S4†), excluding their significant aggregation in the solution phase.¹³ ¹H NMR titrations in CD₃CN/DMSO-*d*₆ mixtures of varying compositions show that the thioureido –NH^d protons are much less accessible by the hydrogen bonding component DMSO-*d*₆ than those of –NH^a, –NH^b and –NH^c protons (Fig. S5†). This means that –NH^d is protected by

an intramolecular hydrogen bond, and thus, it is an indication of the existence of the β -turn structure.³¹ This is also supported by their CD spectra in CH₃CN, which confirm the transfer of the chirality of the alanine residue to the phenylthiourea chromophore in *L*-SAP and the thienylthiourea chromophore in *L*-PAS, by the observed CD signals around 280 nm from these achiral chromophores (Fig. 3b).^{21,22} CD bands at 250 nm of *L*-SAP and at 238 nm of *L*-PAS are assigned to the *N*-terminal thiophenecarboxamide and benzamide moieties, respectively. Enantiomeric *D*-SAP and *D*-PAS samples show mirror-imaged CD spectra to those of *L*-SAP and *L*-PAS, respectively (Fig. S6†). This shows that the CD signals are real and the chirality originates from the alanine residue. CD profiles in CH₃CN also differ very much from those in the crystal state (Fig. 3), suggesting their monomer form in CH₃CN in contrast to the well-organized helix structure in the solid state.

Conclusions

In conclusion, our success in building supramolecular helices in the crystal state from folded short azapeptides containing a thiophene moiety demonstrates that chalcogen bonding is capable of driving the formation of a supramolecular helix. *L*-SAP that contains a thiophene moiety at its *N*-terminus forms a supramolecular *M*-helix *via* intermolecular S...S chalcogen bonding between thiophene and thiourea moieties of the neighbouring molecules. *L*-PAS with a thiophene group at the *C*-terminus however forms a *P*-helix of opposite handedness *via* S...O chalcogen bonding between thiophene and amino acid amide groups of alternate molecules next to each other. Our results would thus promote extended investigations of using chalcogen bonding in creating supramolecular helices of diverse structures in both the solid state and solution phase.

Conflicts of interest

There are no conflicts to declare.

Acknowledgements

We greatly appreciate the support of this work by the NSF of China (grant nos. 21820102006, 91856118, and 21521004), the MOE of China through the Program for Changjiang Scholars and Innovative Research Team in University (grant no. IRT13036), and the scientific and technological developing project in Xiamen (grant no. 3502Z20203025).

Notes and references

- C. B. Aakeroy, D. L. Bryce, G. R. Desiraju, A. Frontera, A. C. Legon, F. Nicotra, K. Rissanen, S. Scheiner, G. Terraneo, P. Metrangolo and G. Resnati, *Pure Appl. Chem.*, 2019, **91**, 1889–1892.
- R. Weiss, C. Schlierf and K. Schloter, *J. Am. Chem. Soc.*, 1976, **98**, 4668–4669.
- R. Desiraju Gautam, P. S. Ho, L. Kloo, C. Legon Anthony, R. Marquardt, P. Metrangolo, P. Politzer, G. Resnati and K. Rissanen, *Pure Appl. Chem.*, 2013, **85**, 1711–1713.
- D. J. Pascoe, K. B. Ling and S. L. Cockroft, *J. Am. Chem. Soc.*, 2017, **139**, 15160–15167.
- L. Vogel, P. Wonner and S. M. Huber, *Angew. Chem., Int. Ed.*, 2019, **58**, 1880–1891.
- G. Cavallo, P. Metrangolo, R. Milani, T. Pilati, A. Priimagi, G. Resnati and G. Terraneo, *Chem. Rev.*, 2016, **116**, 2478–2601.
- L. C. Gilday, S. W. Robinson, T. A. Barendt, M. J. Langton, B. R. Mullaney and P. D. Beer, *Chem. Rev.*, 2015, **115**, 7118–7195.
- A. Mukherjee, S. Tothadi and G. R. Desiraju, *Acc. Chem. Res.*, 2014, **47**, 2514–2524.
- A. Brown and P. D. Beer, *Chem. Commun.*, 2016, **52**, 8645–8658.
- A. V. Jentzsch, D. Emery, J. Mareda, S. K. Nayak, P. Metrangolo, G. Resnati, N. Sakai and S. Matile, *Nat. Commun.*, 2012, **3**, 905.
- V. N. G. Lindsay, W. Lin and A. B. Charette, *J. Am. Chem. Soc.*, 2009, **131**, 16383–16385.
- G. Gong, S. Lv, J. Han, F. Xie, Q. Li, N. Xia, W. Zeng, Y. Chen, L. Wang, J. Wang and S. Chen, *Angew. Chem., Int. Ed.*, 2021, **60**, 14831–14835.
- C.-Z. Liu, S. Koppireddi, H. Wang, D.-W. Zhang and Z.-T. Li, *Angew. Chem., Int. Ed.*, 2019, **58**, 226–230.
- J. Cao, X. Yan, W. He, X. Li, Z. Li, Y. Mo, M. Liu and Y.-B. Jiang, *J. Am. Chem. Soc.*, 2017, **139**, 6605–6610.
- X. Yan, K. Zou, J. Cao, X. Li, Z. Zhao, Z. Li, A. Wu, W. Liang, Y. Mo and Y. Jiang, *Nat. Commun.*, 2019, **10**, 3610.
- X. Yan, J. Cao, Y. Zhang, P. Weng, D. Miao, Z. Zhao, Z. Li and Y.-B. Jiang, *Chem. Commun.*, 2021, **57**, 1802–1805.
- P. Scilabra, G. Terraneo and G. Resnati, *Acc. Chem. Res.*, 2019, **52**, 1313–1324.
- J. Y. C. Lim, I. Marques, A. L. Thompson, K. E. Christensen, V. Félix and P. D. Beer, *J. Am. Chem. Soc.*, 2017, **139**, 3122–3133.
- S. Benz, M. Macchione, Q. Verolet, J. Mareda, N. Sakai and S. Matile, *J. Am. Chem. Soc.*, 2016, **138**, 9093–9096.
- P. Wonner, L. Vogel, M. Düser, L. Gomes, F. Kniep, B. Mallick, D. B. Werz and S. M. Huber, *Angew. Chem., Int. Ed.*, 2017, **56**, 12009–12012.
- X.-S. Yan, K. Wu, Y. Yuan, Y. Zhan, J.-H. Wang, Z. Li and Y.-B. Jiang, *Chem. Commun.*, 2013, **49**, 8943–8945.
- X.-S. Yan, H. Luo, K.-S. Zou, J.-L. Cao, Z. Li and Y.-B. Jiang, *ACS Omega*, 2018, **3**, 4786–4790.
- M. M. Bader, R. Custelcean and M. D. Ward, *Chem. Mater.*, 2003, **15**, 616–618.
- P.-T. T. Pham and M. M. Bader, *Cryst. Growth Des.*, 2014, **14**, 916–922.
- E. Navarro-García, B. Galmés, M. D. Velasco, A. Frontera and A. Caballero, *Chem. – Eur. J.*, 2020, **26**, 4706–4713.

- 26 O. Koch, *Mol. Inf.*, 2012, **31**, 624–630.
- 27 C.-I. Brändén and J. Tooze, *Introduction to Protein Structure*, Garland Publishing, New York, 1999.
- 28 A. M. Brückner, P. Chakraborty, S. H. Gellman and U. Diederichsen, *Angew. Chem., Int. Ed.*, 2003, **42**, 4395–4399.
- 29 U. Rost, C. Steinem and U. Diederichsen, *Chem. Sci.*, 2016, **7**, 5900–5907.
- 30 M. Xu, L. Liu and Q. Yan, *Angew. Chem., Int. Ed.*, 2018, **57**, 5029–5032.
- 31 G. T. Copeland, E. R. Jarvo and S. J. Miller, *J. Org. Chem.*, 1998, **63**, 6784–6785.